

Crystal structure of $\text{Ba}_2\text{Li}_{2/3}\text{Ti}_{16/3}\text{O}_{13}$

Christian Dussarrat,^a R. Alan Howie,^b Glenn C. Mather,^b Leticia M. Torres-Martinez^c and Anthony R. West^b

^aInstitut de Chimie de la Matière Condensée de Bordeaux, Château Brivazac, Avenue du Dr. Albert Schweitzer, 33608 Pessac CEDEX, France

^bDepartment of Chemistry, University of Aberdeen, Meston Walk, Old Aberdeen, Aberdeen, Scotland, UK AB24 3UE

^cUniversidad Autonoma de Nuevo Leon, Facultad de Quimica, San Nicolas de los Garza, Mexico

Single crystals of $\text{Ba}_2\text{Li}_{2/3}\text{Ti}_{16/3}\text{O}_{13}$ have been isolated and its crystal structure solved from X-ray diffraction data. The structure is similar to that of $\text{Ba}_2\text{Ti}_6\text{O}_{13}$ and $\text{Na}_2\text{Ti}_6\text{O}_{13}$ [monoclinic, space group $C2/m$ (no.12), $a = 15.171(13)$, $b = 3.8992(18)$, $c = 9.106(4)$ Å, $\beta = 98.64(6)^\circ$, $Z = 2$], but one of the three independent octahedral sites contains partial substitution of Ti by Li, whereas the others are uniquely occupied by Ti. This phase contains only Ti^{4+} , in contrast to $\text{Ba}_2\text{Ti}_6\text{O}_{13}$, which has a mixture of Ti^{3+} and Ti^{4+} . The structure is described in terms of both an octahedral framework and a cubic close-packing model of $[\text{Ba}_2\Box\text{O}_{13}]$ layers (\Box : vacancy).

The $\text{BaO-Li}_2\text{O-TiO}_2$ system is currently of interest due to the discovery of two phases which show relatively high Li^+ -ion conductivity. One is a hollandite-like phase, $\text{Ba}_{3x}\text{Li}_{2x+4y}\text{Ti}_{8-2x-y}\text{O}_{16}$,¹ the other is of uncertain composition but shows good conduction properties.² Recently, Torres-Martinez *et al.* have carried out a phase diagram study of the ternary system $\text{BaTiO}_3\text{-Li}_2\text{TiO}_3\text{-TiO}_2$, in which a number of ternary phase regions were established.³ A significant region of $\text{Ba}_4\text{Ti}_{13}\text{O}_{30}$ ternary solid solution and a smaller area of $\text{BaTi}_5\text{O}_{11}$ were found. Other single-phase areas included a region centred on the Li^+ -ion conducting hollandite-like phase, a phase centred on $\text{BaLi}_2\text{Ti}_6\text{O}_{14}$, a phase based on a previously reported solid solution $\text{Ba}_2\text{Ti}_{10-x}\text{Li}_4\text{O}_{22}$ ⁴ and a new phase which formed over a range of compositions close to the composition $\text{Ba}_3\text{Li}_2\text{Ti}_8\text{O}_{20}$. As a consequence of the crystal structure studies reported here, the actual composition of this latter phase is found to be $\text{Ba}_2\text{Li}_{2/3}\text{Ti}_{16/3}\text{O}_{13}$. Its crystal structure is discussed with reference to a series of titanate phases of general formula $\text{A}_m\text{M}_{2n}\text{O}_{4n+1}$ (A = alkali-metal, alkaline-earth metal, M = octahedrally coordinated cation), and is also compared with a number of similar structures in which the octahedral cation composition is different to that of the title phase.

Experimental

Needle-shaped single crystals of the title phase were prepared by heating an intimate mixture of TiO_2 and BaCO_3 in 8:3 molar ratio with an excess of Li_2CO_3 for one week at 1250°C ; the product was then slow-cooled to room temperature at a rate of 5°C h^{-1} . A crystal suitable for single-crystal analysis was selected from the reaction mixture under a petrographic microscope. Details of the data collection are summarised in Table 1. The atomic coordinates for $\text{Ba}_2\text{Ti}_6\text{O}_{13}$ were adopted as the starting point for the refinement,⁸ which was carried out by full-matrix least squares. On refinement, it became clear that Ti(2) had a high (isotropic) thermal vibration parameter compared with Ti(1) and Ti(3) and it was concluded that the Ti(2) site had undergone significant substitution of Li for Ti, compatible with the preparation conditions of the material. The refinement was then completed with variable occupancies of the Ti(2) site. All atoms were refined anisotropically, except for O(6) and O(7) which became non-positive definite when this was attempted. A further anomaly, discussed below, is the presence in the final difference map of rather large residual maxima. Refinement conditions and final reliability factors are

given in Table 1. Atomic coordinates and bond distances are summarised in Tables 2 and 3, respectively.†

Results and Discussion

The crystal structure of $\text{Ba}_2\text{Li}_{2/3}\text{Ti}_{16/3}\text{O}_{13}$ is essentially analogous to that of $\text{Na}_2\text{Ti}_6\text{O}_{13}$ and $\text{Ba}_2\text{Ti}_6\text{O}_{13}$. The Ti(1)O₆, Ti/Li(2)O₆ and Ti(3)O₆ octahedra form edge-sharing trimers, as shown in Fig. 1. These trimers corner-share with other trimers to form layers parallel to the ac plane. Between successive layers, the trimers edge-share forming infinite ribbons with a zigzag arrangement which run parallel to b . A projection of the structure along the b -axis is shown in Fig. 2. The Ba atoms are found within the tunnels which are formed between these ribbons of edge-sharing octahedra.

The structure may also be described by a close-packing model in which $[\text{Ba}_2\Box\text{O}_{13}]$ layers form a cubic close-packed array. The Li and Ti cations lie in interstices between the close-packed layers. Fig. 3 shows the $[\text{Ba}_2\Box\text{O}_{13}]$ layers which lie parallel to the $(5-1-1)$ planes of the unit cell. Barium is eleven-coordinate as a result of the oxygen vacancy in the $[\text{Ba}_2\Box\text{O}_{13}]$ layer which, if occupied, would confer a twelve-coordinate cuboctahedral coordination on Ba, equivalent to the A-cation environment in the cubic perovskite structure. Fig. 4 shows the coordination environment of Ba; it is composed of an antiprism of oxygens together with five oxygens which lie in a $[\text{Ba}_2\Box\text{O}_{13}]$ layer.

All three octahedra are distorted; the greatest distortion occurs for Ti(3)O₆, in which the bond distances are spread over the range 1.805 to 2.207 Å. A large variation of Ti-O distances is not uncommon in barium titanates, and is the result of the surrounding O atoms experiencing differing bond strengths.⁹ The mean Ti-O distance, 1.982 Å, is similar to that found in most barium titanates. Similarly, the range of Ba-O distances, 2.696–3.224 Å, falls within the limits of Ba-O distances found in barium titanates.

As mentioned previously, there are sizeable residual maxima in the final difference map. One of these, $2.6 \text{ e } \text{Å}^{-3}$ in size, is situated at 0.84 Å from Ba and is attributable to ripple. The other, $3.7 \text{ e } \text{Å}^{-3}$ and 1.95 Å from Ba, and almost directly above

† Atomic coordinates, thermal parameters, and bond lengths and angles have been deposited at the Cambridge Crystallographic Data Centre (CCDC). See Information for Authors, *J. Mater. Chem.*, 1997, Issue 1. Any request to the CCDC for this material should quote the full literature citation and the reference number 1145/46.

Table 1 Crystallographic data

crystal data	
Ba ₂ Li _{2/3} Ti _{16/3} O ₁₃	$D_c = 4.631 \text{ Mg m}^{-3}$
$M_r = 742.76$	Mo-K α radiation
monoclinic	$\lambda = 0.71073 \text{ \AA}$
space group $C2/m$	cell parameters from 14 reflections
$a = 15.171(13) \text{ \AA}$	$\theta = 7.7\text{--}14.5^\circ$
$b = 3.8992(18) \text{ \AA}$	$\mu = 10.6 \text{ mm}^{-1}$
$c = 9.106(4) \text{ \AA}$	$T = 298 \text{ K}$
$\beta = 98.64(6)^\circ$	platey needle
$V = 532.5(6) \text{ \AA}^3$	$0.30 \times 0.12 \times 0.04 \text{ mm}$
$Z = 2$	colourless
data collection	
Nicolet P3 diffractometer	$h = -18 \rightarrow 18$
θ - 2θ scans	$k = 0 \rightarrow 5$
absorption correction: ψ -scans ⁵	$l = 0 \rightarrow 12$
$T_{\min} = 0.535$, $T_{\max} = 0.648$	908 measured reflections
908 reflections with $F > 4\sigma(F)$, $n = 4$	855 independent reflections
$R_{\text{int}} = 0.027$	frequency: 1 in 50
$\theta_{\max} = 30^\circ$	
refinement	
refinement on F	program used to refine structure: SHELX-76. ⁷
$R = 0.052$	$w = 1/(\sigma^2 F + 0.0003 F^2)$
$wR = 0.048$	$(\Delta/\sigma)_{\max} = 0.001$
GOF = 2.092	$\Delta\rho_{\max} = 3.74^a$, 2.62^b
776 reflections	$\Delta\rho_{\min} = -4.64$
61 parameters	isotopic extinction coefficient (SHELX76) ^{7a}
data collection and cell refinement: Nicolet P3 software. ⁶	scattering factors from ref. 7(b)

^a1.95 Å from Ba, i.e. at $x, \frac{1}{2} + y, z$ relative to Ba at x, y, z . ^b0.84 Å from Ba. ^cStandard check frequency.

Table 2 Atomic coordinates ($\times 10^4$) and thermal parameters ($\times 10^3$) for Ba₂Li_{2/3}Ti_{16/3}O₁₃ with e.s.d.s in parentheses^a

atom	x/a	y/b	z/c	U_{eq}^b	occupancy
Ba ^c	514.8(6)	0	7676.7(8)	8.9(2)	
Ti(1)	3802(2)	0	9056(2)	7.9(6)	
Ti(2)	2583(2)	0	2284(3)	3.6(9)	0.640(13)
Li(2)	2583(2)	0	2284(3)	3.6(9)	0.360(13)
Ti(3)	3301(2)	0	5613(2)	4.9(6)	
O(1)	1306(8)	0	1091(10)	13(2)	
O(2)	2633(6)	0	7606(10)	6(2)	
O(3)	2010(6)	0	4313(9)	6(2)	
O(4)	3334(7)	0	845(10)	10(2)	
O(5)	3724(8)	0	3863(11)	15(2)	
O(6)	4292(7)	0	7022(10)	10(2)	
O(7)	5000	0	10000	16(3)	

^aAll sites are fully occupied unless otherwise stated. ^b $U_{\text{eq}} = 1/3 \sum_i \sum_j U_{ij}$. ^cAll atoms are in position 4i, apart from O(7) which is in 2b of space group $C2/m$.

Table 3 Bond distances (Å) for Ba₂Li_{2/3}Ti_{16/3}O₁₃

Ti(1)–O(1)	1.9594(11)	Li/Ti(2)–O(1)	2.074(12)
Ti(1)–O(2)	2.046(9)	Li/Ti(2)–O(2)	1.8920(18) × 2
Ti(1)–O(4)	1.873(9) × 2	Li/Ti(2)–O(3)	2.157(9)
Ti(1)–O(6)	2.096(10)	Li/Ti(2)–O(4)	1.861(10)
Ti(1)–O(7)	1.890(2)	Li/Ti(2)–O(5)	2.077(11)
Ti(3)–O(2)	2.207(9)	Ba–O(1)	3.160(9)
Ti(3)–O(3)	2.130(9)	Ba–O(1)	3.133(11)
Ti(3)–O(3)	2.009(3) × 2	Ba–O(2)	3.224(10)
Ti(3)–O(5)	1.805(10)	Ba–O(4)	2.820(7) × 2
Ti(3)–O(6)	1.824(10)	Ba–O(5)	2.755(8) × 2
		Ba–O(6)	2.696(7) × 2
		Ba–O(7)	3.0632(6) × 2

Ba in the direction of b , is not so easy to explain. One plausible explanation is that it results as a consequence of stacking faults in the creation of the layers perpendicular to b . The Li and Ti occupancy factors for the shared site [0.360(13) and 0.640(13), respectively] suggest that the composition of the material is slightly Li rich compared with the ideal where all

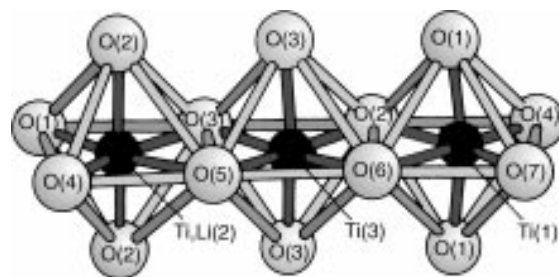


Fig. 1 Cation arrangement in trimer of edge-sharing octahedra

sites are fully occupied with occupancies of 1/3 and 2/3, respectively. The discrepancy is, however, only about $2 \times \text{e.s.d.}$ and may not be significant. It was not feasible to carry out direct chemical analysis of the crystal, especially of its Li content and so some slight ambiguity remains over the precise composition and structural model.

The stoichiometry of the title phase, Ba₂Li_{2/3}Ti_{16/3}O₁₃, differs in its Li (and O) content from that proposed previously, Ba₃Li₂Ti₈O₂₀, but the Ba:Ti ratio is the same. This indicates that loss of Li₂O by volatilisation can be a significant problem during high temperature syntheses. This phase may exist over a limited stoichiometry range as indicated previously;³ one possibility is to have partial reduction of Ti⁴⁺ according to $\text{Li}^+ + 2\text{Ti}^{4+} \rightleftharpoons 3\text{Ti}^{3+}$. This mechanism would retain full occupancy of the octahedral sites, as is found in isostructural Ba₂Ti₆O₁₃.⁸ We think this mechanism to be unlikely in the non-reducing conditions used here, however.

Two other means of creating non-stoichiometry can be imagined, assuming full occupancy of oxygen positions and the cation oxidation states to be +2(Ba), +1(Li), +4(Ti). (1) A replacement mechanism $4\text{Li}^+ \rightleftharpoons \text{Ti}^{4+}$, with creation of vacancies on the octahedral sites, consistent with the structure of isostructural Ba₂Ti_{5.5}O₁₃.¹⁰ (2) A slight substoichiometry in barium sites ($4\text{Ba}^{2+} \rightleftharpoons 4\text{Li}^+ + \text{Ti}^{4+}$) constrained by the limit of full occupancy of the octahedral sites. Then, similarly to the hollandite-like phase, Ba_{3x}Li_{2x+4y}Ti_{8-2x-2y}O₁₆,¹ a general

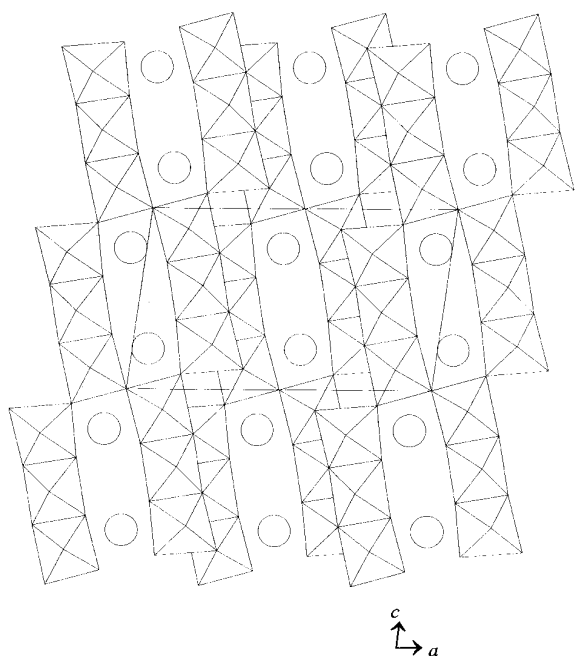


Fig. 2 Projection of the Ba₂Li_{2/3}Ti_{16/3}O₁₃ structure along *b*. Ba atoms are represented as circles.

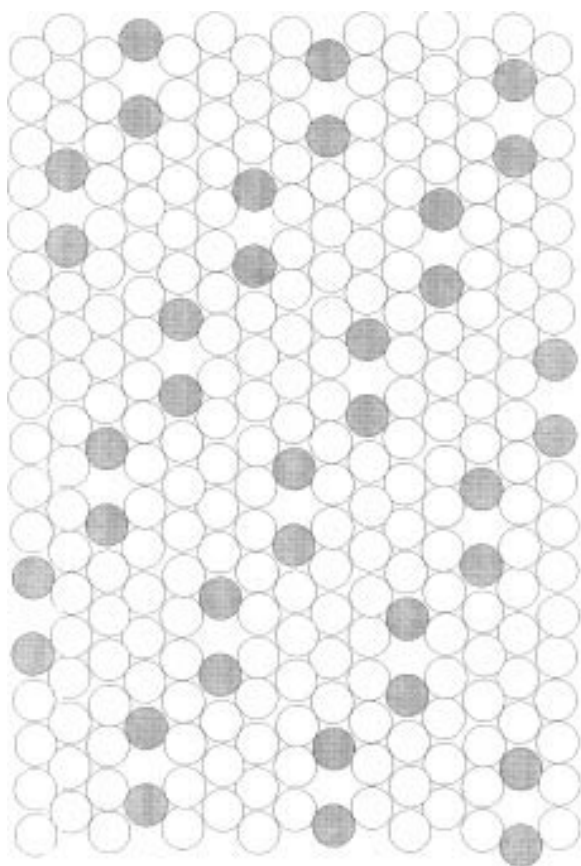


Fig. 3 A close-packing layer of composition [Ba₂□O₁₃] where □ is a vacancy. Ba atoms are shown as shaded circles.

formula covering the solid solution area can be written Ba_{2-x}Li_{2/3+x-4y}Ti_{16/3+x/4+y}O₁₃.

The results of this structure determination point to a comparatively simple explanation of the ease of preparation of this variant of the Ba₂Ti₆O₁₃ structure type, namely the substitution

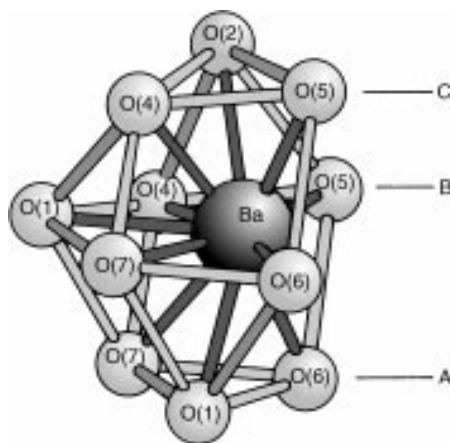


Fig. 4 Coordination environment of Ba

of Li for Ti apparently exclusively in the Ti(2) site. In this way, charge balance is attained without the need for any reduction of Ti⁴⁺ to Ti³⁺. A number of other structurally related phases show variations in the occupancies of the octahedral sites. In isostructural Ba₂Ti_{5.5}O₁₃, for example, the departure from the ideal composition is accommodated by the presence of vacancies in the central octahedron of the trimeric unit.¹⁰ A small number of phases with more than one type of octahedrally coordinated cation have been reported. In the case of Ba₂Fe₂Ti₄O₁₃,¹¹ Fe and Ti are distributed over all three octahedral sites, although Fe shows a strong preference for one of the end sites in the trimer of octahedra. The octahedral cation site distribution in Ba₂Ti₄Cr₂O₁₃ could not be determined unambiguously by XRD due to the similar scattering factors of Cr³⁺ and Ti⁴⁺.¹² Lattice energy calculations, nevertheless, predict that Cr³⁺ would prefer an end site in order to minimize Coulombic cation-cation repulsion effects. In Ba₂Ti₅ZnO₁₃, there is also a preference for Zn to occupy an end site in the trimer.¹³ As far as we are aware, Ba₂Li_{2/3}Ti_{16/3}O₁₃ is the only analogue in which the non-titanium cation occupies a single crystallographic site; in the others, with the possible exception of the Cr analogue, the two octahedral cations are distributed, but non-statistically, over more than one site. The Li⁺ ions are, thus, isolated and in fully occupied sites. This would appear to explain why Ba₂Li_{2/3}Ti_{16/3}O₁₃ shows no significant levels of Li⁺-ion conduction.

The crystal structure of Ba₂Li_{2/3}Ti_{16/3}O₁₃ belongs to a series of titanates characterised by the formula A_mM_{2n}O_{4n+1}, where A is an alkali-metal or alkaline-earth metal cation which fills a large (ten- or eleven-coordinate) site and M is an octahedrally coordinated cation. These titanates may be thought of as a series of tunnel structures built up from a network of Ti-containing octahedra. In general, *m* is equal to *n*/2 or (*n*+1)/2 for *n* even or odd, respectively, in order to minimize cation-cation interactions in the tunnels. For all members of this series, octahedra share edges within a layer, creating a unit which is *n* octahedra wide. Each octahedral unit shares corners with two other units in the same layer and edges with units in the layers above and below, to form a network of infinite chains of edge-sharing octahedra; these chains have a zigzag arrangement and are parallel to the *b* direction of the unit cell. The large A cations are found in the tunnels which are formed by the network of infinite chains. The *b* parameter corresponds approximately to the diagonal of an octahedron (*i.e.* the width of a layer) and is about 3.7–3.8 Å in every structure of the series (Table 4). The size of the *a* parameter is approximately 15 Å in every structure, with the exception of Cs_{0.61}Ti_{1.844}O₄. In this instance, the large size of caesium results in an *a* parameter that is greater than expected. Only the *c* parameter

Table 4 Unit-cell parameters and space group for members of the series $A_nM_{2n}O_{4n+1}$

n	phase	space group	$a/\text{\AA}$	$b/\text{\AA}$	$c/\text{\AA}$	$\beta/^\circ$	ref.
2^a	BaTi ₄ O ₉	<i>C2/m</i>	14.77	3.79	6.29	100.3	9
$2+3^b$	K ₂ SrTi ₁₀ O ₂₂	<i>C2/m</i>	15.317	3.787	15.439	102.68	15
3	Ba ₂ Li _{2/3} Ti _{16/3} O ₁₃	<i>C2/m</i>	15.17	3.90	9.11	98.64	this work
$3+4^c$	Na ₂ Ti ₇ O ₁₅	<i>C2/m</i>	14.90	3.74	20.9	96.5	16
4	K ₂ Ti ₈ O ₁₇	<i>C2/m</i>	15.678	3.775	11.991	95.67	14
∞	CS _{0.61} Ti _{1.844} O ₄	<i>Immm</i>	17.012	3.829	2.962	90	17

^aBaTi₄O₉ is a hypothetical structure. ^bIntergrowth between the members $n=2$ and $n=3$. ^cIntergrowth between the members $n=3$ and $n=4$.

depends on the number of octahedra in the units and corresponds to the distance between opposite corners in a unit. Assuming the octahedra are regular, the length of c can be estimated from the relation: $c = \sqrt{2(n^2 + 1)}d_{M-O}$.

References

- C. Suckut, R. A. Howie, A. R. West and L. M. Torres-Martinez, *J. Mater. Chem.*, 1992, **2**, 993.
- W. J. Zheng, R. Okuyuma, T. Esaka and H. Iwahara, *Solid State Ionics*, 1989, **35**, 235.
- L. M. Torres-Martinez, C. Suckut, R. Jimenez and A. R. West, *J. Mater. Chem.*, 1994, **4**, 5.
- E. Tillmanns and I. Wendt, *Z. Kristallogr.*, 1976, **144**, 16.
- A. C. T. North, D. C. Phillips & F. S. Mathews, *Acta Crystallogr., Sect. A*, 1968, **24**, 251.
- Nicolet P3/R3 Data Collection Operator's Manual, Nicolet XRD Corporation, 1980.
- (a) G. M. Sheldrick, SHELX-76 Program for Crystal Structure Determination, University of Cambridge, 1976; (b) *International Tables for X-Ray Crystallography*, Kynock Press, Birmingham, 1974, vol. 4.
- W. H. Baur, E. Tillmanns and W. Hofmeister, *Crystal Struct. Commun.*, 1982, **11**, 2021.
- E. Tillmanns, W. Hofmeister and W. H. Baur, *J. Solid State Chem.*, 1985, **58**, 14.
- V. W. Hofmeister and E. Tillmanns, *Acta Crystallogr., Sect. B*, 1979, **35**, 1590.
- T. A. Vanderah, Q. Huang, W. Wong-Ng, B. C. Chakoumakos, R. B. Goldfarb, R. G. Geyer, J. Baker-Jarvis, R. S. Roth and A. Santoro, *J. Solid State Chem.*, 1995, **120**, 121.
- S. Möhr and Hk. Müller-Buschbaum, *Z. Naturforsch. Teil B*, 1994, **49**, 911.
- R. S. Roth, C. J. Rawn, C. J. Lindsay and W. Wong-Ng, *J. Solid State Chem.*, 1993, **104**, 99.
- M. Le Granvalet and L. Brohan, *J. Solid State Chem.*, 1993, **107**, 127.
- A. D. Wadsley and W. G. Mumme, *Acta Crystallogr., Sect. B*, 1968, **24**, 392.
- T. Sasaki, M. Watanabe, Y. Fujiki, Y. Kitami and M. Yokoyama, *J. Solid State Chem.*, 1991, **92**, 537.
- I. E. Grey, C. Li, I. C. Madsen and J. A. Watts, *J. Solid State Chem.*, 1987, **66**, 7.

Paper 7/03252H; Received 12th May, 1997